CURVE TRACER FOR ELECTROPHYSICAL STUDIES

D. L. Danyuk, I. V. Korotash, and G. V. Pil'ko

UDC 621.317.359.2

A curve tracer for the analysis of the electrophysical properties of superconductors and related structures is described. The curve tracer can record data in a triangle current scan. The output current range ±2 A is determined by the voltage-to-current converter. The control voltage parameters are amplitude ±7.5 V, integral nonlinearity of the triangular voltage < 0.03%, *trigger spike amplitude at the inflection points of the triangular voltage ±350 uV, asymmetry between the rise and fall rates of scanning* < 0.05%. *The scan current has good temperature stability with respect to period and magnitude because only a single reference-voltage source is used. An arbitrary selected region of a characteristic can be scanned both periodically and aperiodically.*

The curve tracer is designed to record current-voltage characteristics and their local peculiarities. It has mostly been used to investigate superconductors by the tunneling spectroscopy technique [1]. The tracer does a bipolar linear current scan across a grounded load. The main components of the device can be used as bias sources U_b for the point tunneling contact [2].

A block diagram of the curve tracer is presented in Fig.1. The source of the control voltage **1** generates the voltage $U_{out} = \tilde{U}_{ref} \sin[\sin^{-1}(U_c t/U_{ref} R_1 C_1)]$ as isosceles triangle without steps, which could lead to magnetic-flux capture by the superconductor sample. Figure 2 shows a circuit diagram of the control voltage supply. The symmetry between the rise and fall rates of U_{out} are better than in [3], and the rate sign can be changed at any moment. This means that a selected portion of a plot can be scanned.

In the generation mode the integrator output voltage $\overline{U}_{out}$ and the inverter output voltage U_{out} at OA_1 and OA_2 outputs, respectively, are in counterphase. The rate of their changes is proportional to the control voltage U_c. The rate signs depend on the state of the Q-output of IC_{6-1}. When it is high, U_c is negative and U_{out} increases while $\overline{U}_{out}$ continues to drop. At the time when $U_{out}=U_{ref}$ the output of OA_4 drives the R-input of IC_{6-1} and sets a low level at the Q-output of IC_{6-1}. Here U_c is positive and U_{out} decreases while $\overline{U}_{out}$ increases. When $U_{out}=U_{ref}$ the OA_5 output drives the S-input of IC_{6-1} and resets the Q-output. This ends the half cycle of the full oscillation. This process is repeated with a period $4R_1C_1U_{ref}/U_c$

Aperiodic variations of the sign rate of U_{out} are initiated by the button B_1. If initially the R-output of IC_{6-2} is high, then switching B_1 pulls the S-input high and changes the Q-output. The leading edge of this pulse across the R_1C_2 circuit affects the C-input and changes the state of IC_{6-1}.

Unit **2** in Fig. 1 is a voltage-to-current converter (VCC) [4]. A simplified circuit diagram of the VCC, which is based on a linear inverting power amplifier, is presented in Fig. 3. The forward transmission circuit consists of an operational amplifier (op-amp) OA_2 and a class B high-power buffer amplifier. Each arm of the

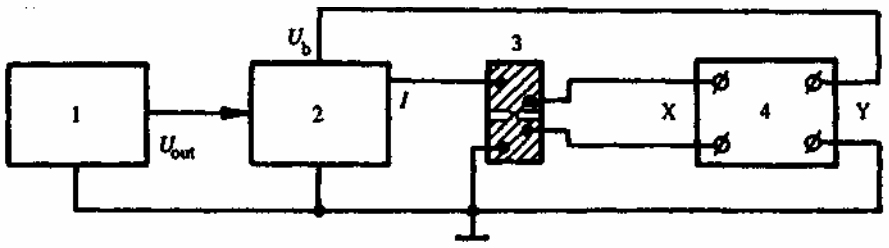

Fig.1. Block diagram of the curve tracer: 1) voltage control supply; 2) voltage-to-current converter; 3) sample; 4) N307 X-Y plotter.

Institute for Metallophysics, Ukrainian Academy of Sciences, Kiev. Translated from *Pribory i Tekhnika Eksperimenta,* No. 6, pp. 186-190, November-December, 1992. Original article submitted October 8, 1991.

 0020-4412/92/3506-1104S12.50

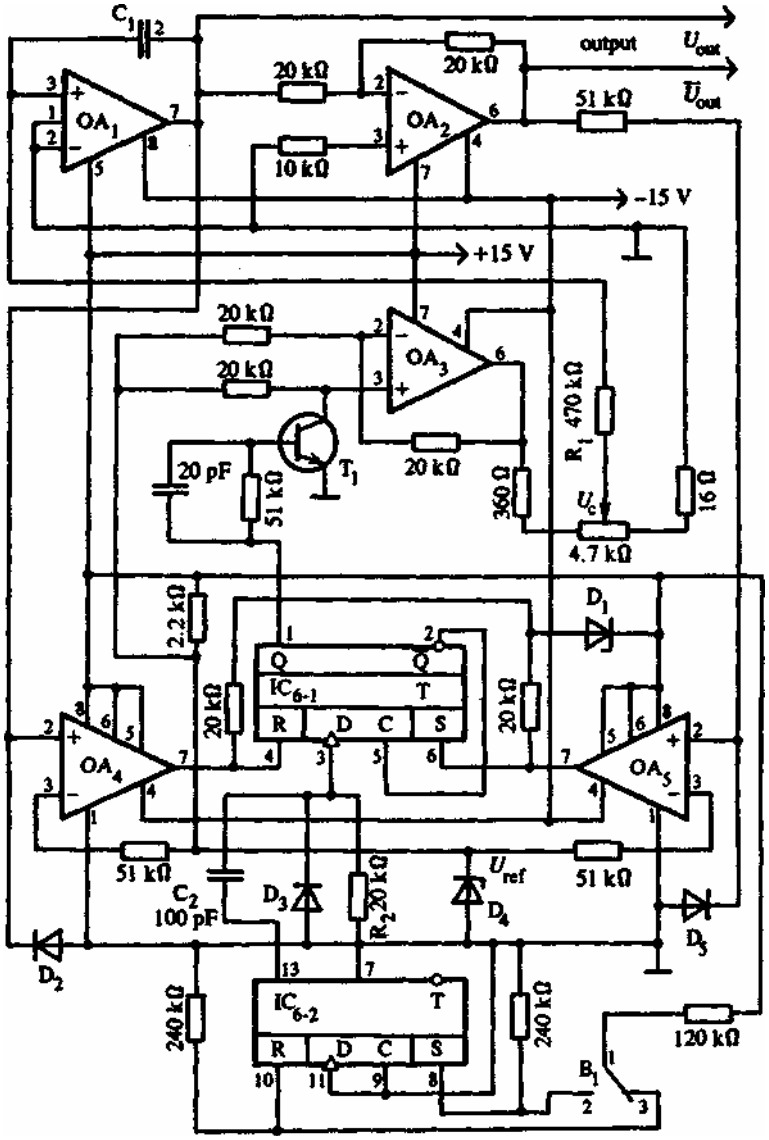

Fig.2. Circuit diagram of the voltage control supply: OA_1) 544UD1A; OA_2 and OA_3) 140UD7; $OA_4$and OA_5) 544SA3A;IC_6) 176TM2; T_1) KT315A; D_1) KC168A; D_2, D_3 and D_6) D311; D_4) D818E.

buffer contains an emitter follower (T_1 and T_4) and an amplifying couple (T_2,T_3 and T_5,T_6) with common voltage feedback (R_1, R_2 and R_3, R_4) and local current feedback formed by the ballast resistors in the emitter circuit of T_2-T_6. The amount of local feedback is chosen by dynamic stability criteria [5]. The voltage gain of each arm is 3.4. The diode D_1 speeds up the base current of T_2 and T_5 when T_1 and T_4 are turned off. Thermal stability is provided by the local feedback and the thermal contact between T_1 and T_2, and T_4 and T_6. The negative feedback is applied to VCC, via the total current feedback (R_8 and OA_1) and the local voltage feedback (R_5-R_7). The load current is converted to a feedback voltage at R_8. Resistor R_8 is selected by a switch which sets the output voltage range. The feedback voltage is transferred via the OA_1 op-amp to the summation junction of the OA_2 op-amp. The inputs of OA_1 are protected by resistive dividers against common-mode input overvoltage. The inverting input divider of OA_1 provides current across R_8 even when the VCC input is disconnected. This sets the output voltage to zero when the input is grounded. The local voltage feedback has the same function.

The reduced conversion error of VCC has three main components. The additive component is determined by the accuracy of resistor R_8 and the transmission ratios of OA_1, and OA_2. It is less than 0.2%. The

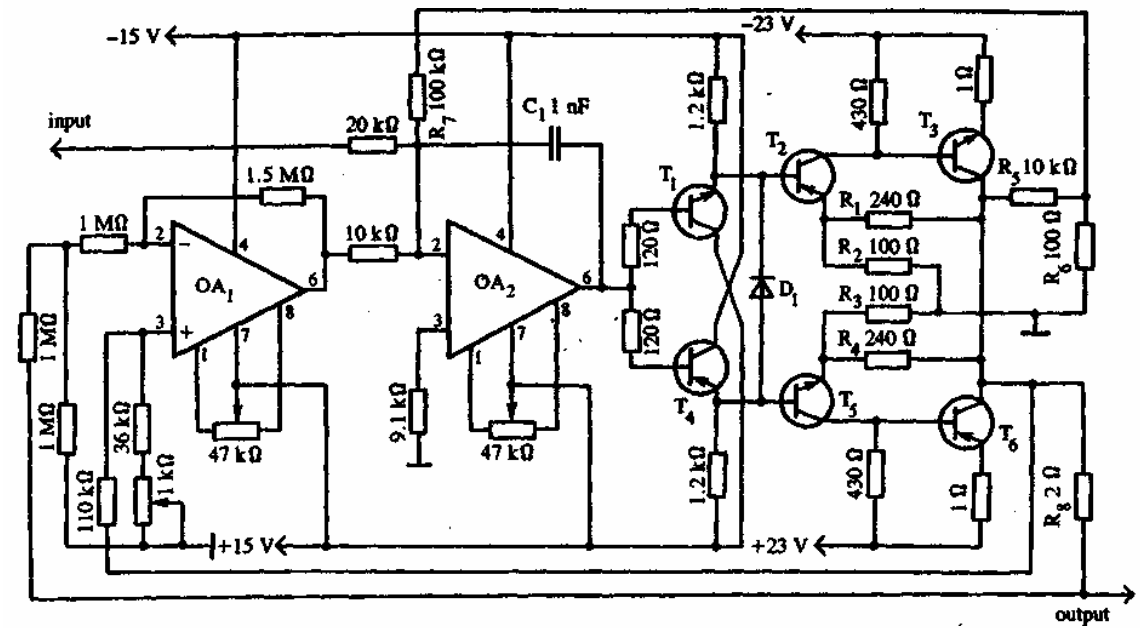

Fig. 3. Circuit diagram of the voltage-to-current converter: OA_1) 544UD1A; OA_2) 140UD6;T_1) KT503D; T_2) KT814B; T_3) KT819B; T_4) KT502A; T_5) KT815B; T_6) KT818B;D_1) D311.

multiplicative component depends on the balance error of the common mode in the differential amplifier OA_1, and is less than 0.1%. The second multiplicative component is produced by the divider current at the OA_1 input. Since the maximum value of this current is under 1.27μA, it contributes an error of less than 0.1% for loads under 20kΩ. The reduced error of the VCC conversion is no more than 0.45%. The main pole of the transfer characteristic is formed by the integrating capacitor C_1. The maximum spike of the transfer characteristic is under 5%.

The VCC is linearized by suppressing the common-mode component in all current shaping sections. To do this only the inverting mode of amplifiers is used in the shaping circuit and in the direct transmission circuit of VCC. This measure permits the error caused by the common-mode to be scaled down by a factor of more than 50 [6]. An additional way of linearizing VCC is multiple-loop feedback applied to the output stage. For short scanning cycles these measures reduce the nonlinearity to well below the intrinsic noise level of the integrator. For long cycles the principal cause of nonlinearity is heat drift in the components and the lack of the loop gain in the stages.

An N307 *X*-*Y* plotter (unit **4**) was used to study the current-voltage characteristics (CVC). The voltage signal was fed to the *X*-input and current signal to the *Y*-input. Oscilloscopes can be used to monitor CVC. To record the CVC derivatives, a differentiating unit was connected between the specimen and the recorder using the technique described in [1], for instance.

A typical example of a curve-tracer operation was the study of microbridges based on the high-T_c superconducting $YBa_2Cu_3O_{7-x}$ ceramics and $YBa_2Cu_3O_{7-x}$ films ~ 1000 Å thick. The films were grown on MgO [100] cleaned surface by the high-frequency magnetron sputtering technique. Microbridges $L \sim 40\mu m$ long and $W \sim 20\mu m$ wide (Fig. 4a) were produced from these films by photolithography and selective etching. The temperature of the superconducting transition was ~ 82.5 °K and to within the accuracy of the measurements were the same for both a film and a bridge. The bridge (see 3 in Fig. 1) was connected by the four-probe technique. Figure 4b displays the microbridge CVC, which was recorded at a temperature of 4.2 °K. In the portions of CVC corresponding to the resistive state around points *A* and *B* as well as in the 06 section (Fig. 4b) there are several singularities. They manifest themselves as variations in the differential resistance of the microbridge resulting from the generation and motion of Abrikosov vortices in the bridge region [7] and by the subharmonics of the material's energy gap. The aperiodic scan mode allowed the *ab* region of the CVC to be presented in a form convenient for consideration (Fig. 4b). The location and shape of the *ab* section

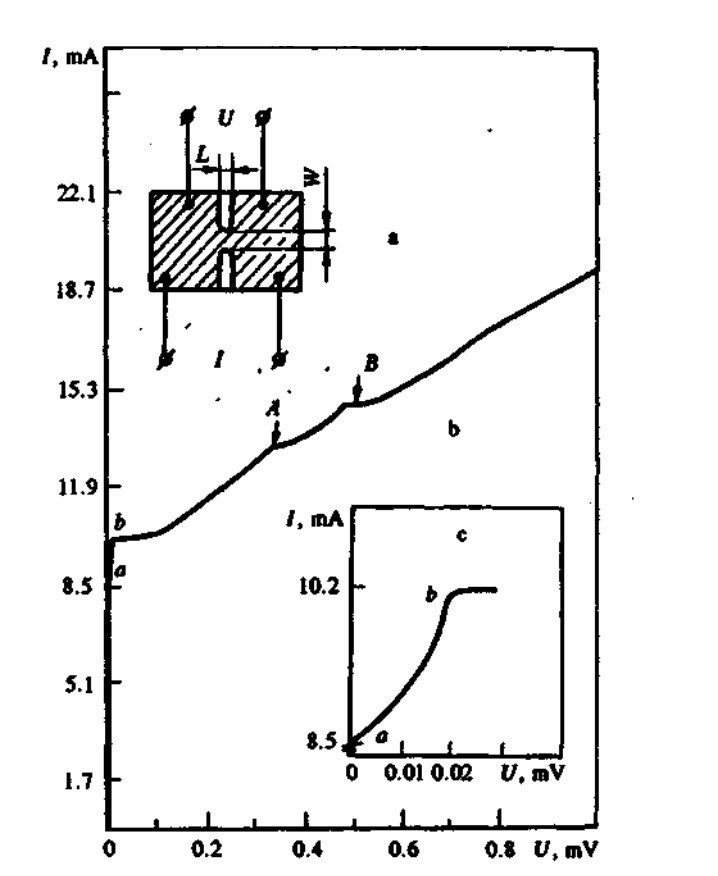

Fig. 4. Current-voltage characteristics of a $YBa_2Cu_3O_{7-x}$ microbridge: a) microbridge specimen; b) current-voltage characteristics; c) the section *ab* of the plot studied by an aperiodic scan.

indicate that its occurrence is determined by the upset of vortex strings under the effect of transfer current. No negative differential resistance is observed in the *ab* section.

Using CVC area scanning we fully utilized the recorder resolution and obtained additional information about the fine structure of the recorded curve. This capability of the curve tracer allowed us to obtain the recent results in studies of high-T_c superconductors [7, 8]. The curve tracer may be used to analyze any function whose argument can be easily presented as a linear function of time.

The experiments were supported by the State program HTSC No. 90050 *Inzhektor.*

LITERATURE CITED

1. I. Vol'f, *Principles of Tunnelling Spectroscopy* [in Russian], Naukova Dumka, Kiev (1990), p. 366.
2. V. S. Edel'man, *Prib. Tekh. Eksp.,* No. 5, 25 (1989).
3. D. L. Danyuk and G. V. Pil'ko, *Prib. Tekh. Ektp.,* No. 1, 115 (1990).
4. D. L. Danyuk and G. V. Pil'ko, *Nauchnoe Priborostroenie* [in Russian], No. 3, 132 (1991).
5. G. V. Pil'ko, Deposited Manuscript No. 6284-B86 [in Russian], Moscow, VINITI (1986), p. 4.
6. E. F. Tailor, *Wireless World,* 83, No. 8, 30 (1977).
7. E. M. Rudenko, I. V. Korotash, I. P. Nevirkovets, et al., *Superconductor Sci. Technol.,* 4, No. 1, 1 (1991).
8. E. M. Rudenko, Yu. M. Boguslavskii, I. P. Nevirkovets, et al., Preprint No. 13 of Institute for Metallophysics, Ukrainian Academy of Sciences, Kiev (1988), p. 58.